5. R. D. SHANNON, J. L. GILLSON and R. J. BOUCHARD, *J. Phys. Chem. Solids* 38 (1977) 877.
6. T. DUPUIS, *Mikrochim. Inchno. Anal. Acta.* (1965) 737.
7. A. J. NOZIK, *Phys. Rev. B* 6 (1972) 453.
8. M. S. WRIGHTSON, D. L. MORSE, A. B. ELLIS, D. S. GINLEY and H. B. ABRAHAMSON, *J. Amer. Chem. Soc.* 98 (1976) 44.

Received 18 September 1978
and accepted 21 February 1979.

K. J. D. MACKENZIE*
W. A. GERRARD
F. GOLESTANI-FARD
Materials and Energy Research Centre,
AryaMehr University of Technology,
P. O. Box 41–2927,
Tehran, Iran

*Present address: Chemistry Division, DSIR, Private Bag, Petone, New Zealand.

The morphology of the aluminium–palladium (Al-rich) eutectic

The aluminium–palladium phase diagram (Al-corner) presents a eutectic at 25 wt% Pd [1] or at 23% Pd [2] at 88 K. A compendium of the most important characteristics of this system, made by the authors on the basis of known data [1, 2] is given in Table I.

As reported in the literature [3], if the structure of this alloy is properly oriented, a high strength is gainable at elevated temperatures (673 K). Moreover, under hot-rolled conditions, it exhibits a fine-grained superplasticity manifested by a substantial elongation (~400%) [4]. However, the structure of this interesting system is not well established and some additional information is needed in order to clarify the doubtful points. For that reason a study was made of the microstructural characteristics under conditions of *in situ*-grown morphology.

The unidirectional solidification technique leads to a much simpler arrangement of the phases in comparison to that achieved under random casting conditions. The results of the research are reported here.

The master alloy was prepared by induction furnace melting (Al_2O_3 crucible) under a positive pressure of argon with the constituent elements mixed in a ratio nominally equal to the eutectic composition: 23 wt% Pd [2]. The base materials were of commercial purity: Al 99.998% and Pd 99.98%. After fusion, the ingot was cleaned and swaged at room temperature into a rod of 8.5 mm final diameter. Seven sections of length 20 cm were obtained and used as a charge for unidirectional solidification trials. Each section of the rod was placed in a cylindrical graphite crucible, remelted and unidirectionally solidified at a constant growth rate. The equipment has been described elsewhere [5]. The solidification rates were respectively: 3.3, 5.6, 6.5, 13.8, 14.7, 41.9 and 73.6 cm $sec^{-1} \times 10^{-4}$, and the thermal gradient was about 100° C cm^{-1}.

The most important morphological features revealed by the metallographic observations (electro-etching in a solution of perchloric acid and acetic acid) are summarized in Table II, together with the corresponding growth rates and also weight compositions determined by chemical analysis. The alloys 1 and 2 were found to be slightly hypo-eutectic. However, such deviations from eutectic compositions are assumed not to have affected the basic microstructure. Chadwick

TABLE I Characteristics of the Al–Pd (Al-rich) eutectic [1, 2]

Solute element	Pd
Composition	23 wt% Pd [2], 25 wt% Pd [1]
Phases	
Matrix	Al (Pd solubility non detectable)
Second phase	Al_3Pd
Eutectic melting point	888 K
Composition	56.9 wt% Pd
Transformation temperature	1058 K
Transformation type	Peritectic
	Liq. (50% Pd) + $Al_3Pd_2 \rightarrow Al_3Pd$
Crystal structure	Orthorhombic
Theoretical density	4580 kg m^{-3} *
Vol. % at eutectic temperature	28.8*

*Calculated by the authors

0022–2461/79/102512–05 $02.50/0

TABLE II Al–Pd (Al-rich) eutectic morphology as function of solidification rate

Alloy no.	Composition (wt % Pd)	Growth rate (cm sec^{-1})	Thermal gradient (° C cm^{-1})	Morphology
1	18.63	3.3×10^{-4}	100	Hypoeutectic. Chinese script micromorphology
2	*	5.6×10^{-4}	>100	As above
3	19.16	6.5×10^{-4}	100	Eutectic. Chinese script micromorphology
4	*	1.38×10^{-3}	>100	Fully eutectic. Sharply angular lamellar micromorphology Cellular macrostructure
5	22.93	1.47×10^{-3}	100	As above
6	22.86	4.19×10^{-3}	100	As above
7	22.75	7.36×10^{-3}	100	As above
Cast structure	22.85	–	–	Chinese script and irregular lamellar

*Not analysed.

[6] has, in fact, shown that a relatively small excess of one component did not alter the lamellar eutectic structure of an Al–Cu alloy. At low growth rates (alloys 1 to 3) the micromorphology can be classified as "Chinese script" type (Fig. 1). The dispersed particles of the second phase occur as lamellae and platelets, which are sharply bent through an angle of 90°. The particles tend to be aligned with respect to each other and are dispersed in groups of different discrete orientations within the overall region of the examined section of the ingot (Fig. 2). The script pattern probably arises from a preferred crystallographic relationship at the interfaces between the matrix and the second phase as it is the case in the most classical example of "Chinese script" eutectic: Mg–Mg_2Sn [7].

At intermediate growth rates (alloys 4 and 5), the morphology changes abruptly and without apparent relation to the previous morphology (Fig. 3). The platelets and lamellae are arranged in regular cells following radial patterns. With increasing growth rates (alloys 6 and 7) the cellular macrostructure becomes stronger with the centre of the cells often composed of particular lamellae which present three branches radiating outward through an angle between plates of 120° (Fig. 4). At the periphery of the cells the plates are thicker than at the centre. This type of morphology was observed previously in other eutectic systems, such as NiAl–Cr(Mo) [8] and Ti–Fe [9]. The two types of morphology, "Chinese script structure" and "angular lamellar" were already present in master ingot structures, although in less simple topological arrangements (Fig. 5). This must be related to a large growth rate spectrum present during random casting solidification; that is without a control over solidification.

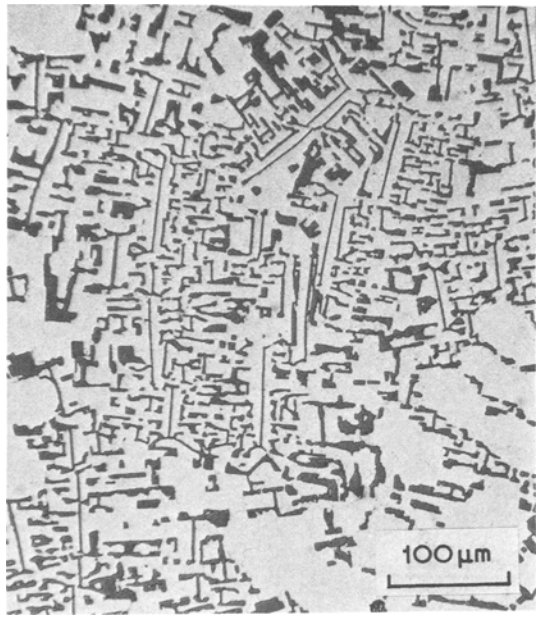

Figure 1 "Chinese script" type structure in the Al–Pd eutectic alloy unidirectionally solidified at a low rate (Alloy 1, transverse section).

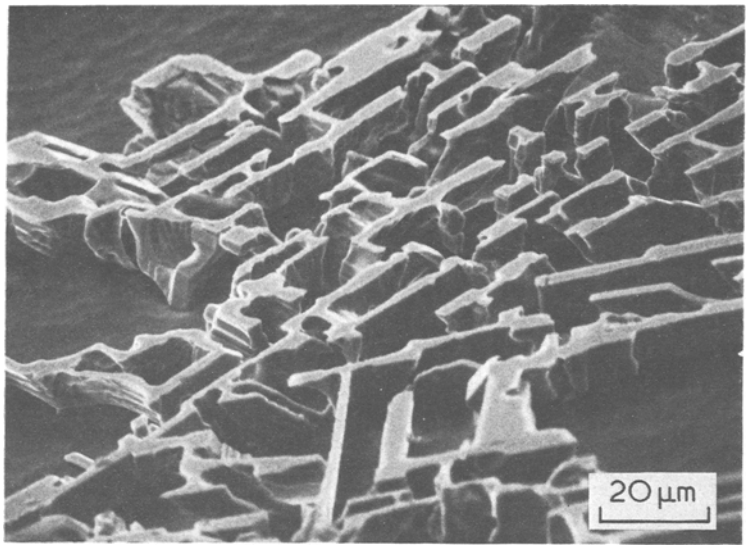

Figure 2 Scanning electron micrograph of the Al–Pd eutectic alloy unidirectionally solidified at a low growth rate (Alloy 1), with the Al matrix removed in order to show the intermetallic phase.

X-ray diffraction investigation (powder method) and chemical analysis performed on second phase particles extracted from solidified bars by dissolution of the Al-matrix by electrochemical attack (perchloric acid) led to identification of two components, namely:

(i) the orthorhombic Al_3Pd [1] present in the alloys having a Chinese script morphology (alloys 1 to 3);

(ii) the intermetallic $Al_{3.89}Pd$, found in the alloys characterized by an angular lamellar morphology (alloys 4 to 7). This compound could be indexed assuming a hexagonal cell with $a = 4.37$ Å, $c = 4.85$ Å ($c/a = 1.109$).

This last phase has a lattice structure similar to that found by Kossowsky and Johnston for the compound Al_3Pd_2 [3]. However, chemical analysis data lead, in our case, to the empirical formula $Al_{3.89}Pd$. This compound is considerably less rich in Pd than Al_3Pd_2 and slightly richer in Pd than the Al_4Pd phase isomorphous with Al_4Rh (monoclinic) reported by [10].

The volume fraction of the second phase, as determined by a Classimat-Leitz Image Analysing Computer on 40 different areas of various samples, is 28.3% for the Chinese-type morphology (alloys 1 to 3) and 44.5% for the angular lamellar microstructure (alloys 4 to 7). In the case of the Chinese script morphology, the measured volume fraction of the second phase corresponds very closely to the theoretical value (28.8%, Table I), calculated assuming for the Al_3Pd compound the orthorhombic crystal structure reported in the literature [1]. For the lamellar microstructure, a good agreement between the measured volume fraction (44.5%) and that calculated (43.0%) is reached, assuming for $Al_{3.89}Pd$ a non-primitive hexagonal or an orthohexagonal unit cell. Unfortunately, a precise determination of the cell structure could not be done because of the absence of large

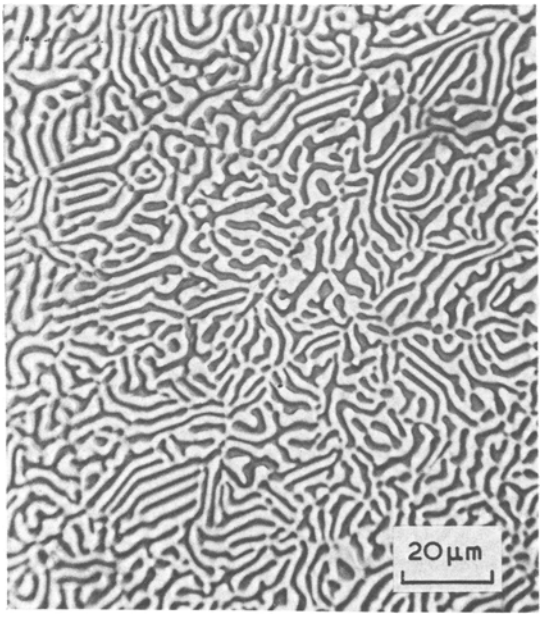

Figure 3 Regular cellular macrostructure and angular lamellar micromorphology in the Al–Pd eutectic alloy unidirectionally solidifed at an intermediate rate (Alloy 4, transverse section).

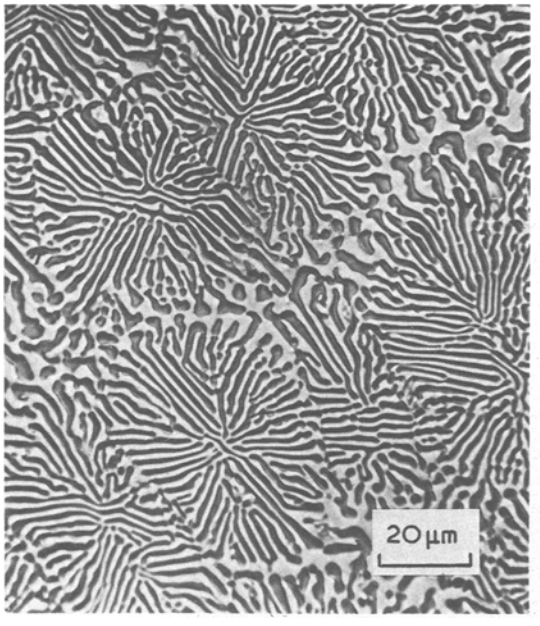

Figure 4 Strong cellular macrostructure and angular lamellar micromorphology in the Al–Pd eutectic alloy unidirectionally solidified at a high rate (Alloy 6, transverse section).

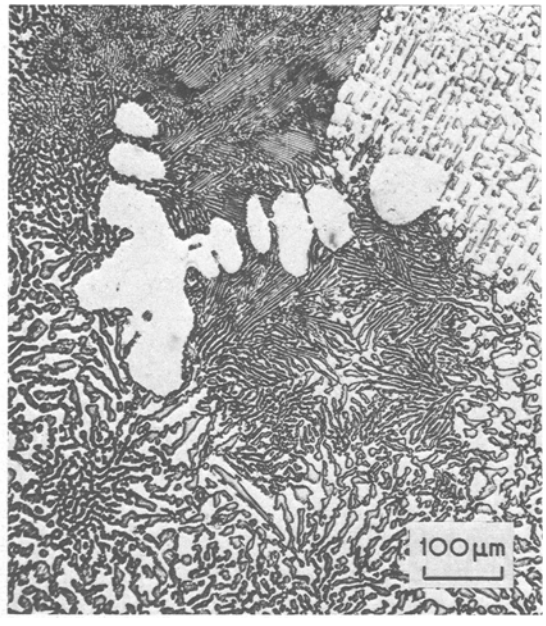

Figure 5 Microstructure of the Al–Pd eutectic (master ingot).

crystals permitting an accurate measurement of the density.

On the basis of the present results the structure seems to depend on two eutectic reactions. At low solidification rate the equilibrium reaction, liquid $\rightarrow Al + Al_3Pd$, occurs. At higher solidification rates the Al_3Pd compound does not precipitate from the melt and there is the establishment of metastable $Al–Al_{3.89}Pd$ eutectic. Complete suppression of the $Al_{3.89}Pd$ compound is possible only by slow cooling. It is very likely also that the imposed temperature gradient in the liquid at the solid–liquid interface has an influence. The high value of $100^\circ C\,cm^{-1}$ of the authors' experiments favours the metastable reaction. A very similar behaviour in eutectic systems by rapid cooling was also observed in Al–Fe alloys. In this case the application of a high solidification rate allowed a metastable eutectic reaction $Al–Al_6Fe$ to occur and also suppression of primary Al_3Fe growth [11].

In conclusion, it was found that the Al–Pd system presents in stable phase equilibrium a eutectic at 23 wt % Pd with an orthorhombic Al_3Pd as a second phase [2]. The system seems also to be characterized by a metastable phase equilibrium, following the solidification conditions. At high growth rates (1.38×10^{-3} to 7.36×10^{-3} cm sec^{-1}) and high thermal gradient in the liquid ($100^\circ C\,cm^{-1}$), a new metastable phase was found (hexagonal $Al_{3.89}Pd$). Finally, the "Chinese script" type morpholgy, previously found in Al–Pd alloys [3, 4], was confirmed.

Acknowledgements

The authors wish to thank Dr Serrini for his technical assistance in chemical analysis. Thanks are also due to Messrs Baranzini, Haine, Misirocchi and Quazzo.

References

1. M. HANSEN and K. ANDERKO, "Constitution of Binary Alloys" (McGraw-Hill Book Co., New York, 1958) p. 124.
2. L. F. MONDOLFO, "Aluminium Alloys: Structure and Properties" (Butterworths, London, 1976). 354.
3. R. KOSSOWSKY and W. C. JOHNSTON, *Trans. AIME* **245** (1969) 1826.
4. G. PIATTI and M. BARDY, *Mater. Sci. Eng.* (submitted).
5. K. N. STREET, F. C. ST. JOHN and G. PIATTI, *J. Inst. Metals* **95** (1967) 326.
6. W. A. CHADWICK, *ibid.* **91** (1962–3) 169.
7. R. W. KRAFT, *Trans. AIME* **227** (1963) 393.
8. H. E. CLINE, J. L. WALTER, E. LIFSHIN and R. R.

RUSSELL, *Met. Trans.* 2 (1971) 189.
9. M. K. THOMAS and R. E. TRABOCCO, Proceedings of the Conference "*In Situ*-Grown Composites", Lakeville, Connecticut (1972) p. 301.
10. A. MAGNELL, L. E. EDSHAMMAR and T. DAGGERMANN, Final technical Report No. 1 under contract DA-91-591-EUC-2734 (AD 426927) (1963) p. 46.
11. C. McL. ADAM, I. O. SMITH and L. M. HOGAN, as for [9], p. 309.

Received 28 November 1978
and accepted 23 March 1979.

G. PIATTI
G. PELLEGRINI
Materials Science Division,
CEC, Joint Research Centre,
Ispra Establishment,
I-21020 Ispra (Va), Italy

The effect of powdering on the polytypic crystal structures of tin disulphide

During a study of polytypism in single crystals of tin disulphide grown by the iodine vapour transport method, single crystal X-ray diffraction studies brought to light several instances of polytypic structure, and in one or two cases revealed hitherto unreported polytypes. A full account of this work is to appear elsewhere [1]. A parallel study of similar samples by means of powder X-ray diffraction failed to reveal any indication of polytypes other than the 2H form [2].

In view of this, it was thought that the process of crushing and grinding in an agate mortar, adopted for the preparation of powder specimens, might be affecting the atomic structure of the resulting samples, possibly by the introduction of numerous stacking faults and dislocations to alter the structure of the higher order polytypes. The structure of tin disulphide is isomorphous with cadmium iodide, and is characterized by easy cleavage and glide parallel to the basal plane of the trigonal crystals.

To test this hypothesis, three SnS_2 crystals were carefully examined by single crystal diffraction methods to discover their polytype structures, and they were then crushed to make powder specimens. The powder diffraction data were then compared with those from the single crystals to determine whether the same polytypes were still present.

The powder data derived from a crystal known from single crystal studies to consist entirely of the 2H polytype ($P\bar{3}m1$; Zhdanov symbol [11], $a = b = 3.643 \pm 0.002$ Å, $c = 5.894 \pm 0.005$ Å) were in excellent agreement with those calculated for the 2H structure. The comparison is made in Table I. Absorption and temperature factor corrections have not been applied, and the relative intensities only of diffraction lines which are fairly close together may be quantitatively compared. The structure of this crystal is therefore unaffected by the powdering process.

TABLE I A comparison of the experimentally observed powder data for SnS_2 crystal no. 1 (2H polytype) with values calculated on the basis of the 2H structure (CuKα radiation)

Reflection hkl	θ_{obs} (deg)	θ_{calc} (deg)	d_{calc} (Å)	I_{calc} (normalized)	I_{obs}
0 0 1	7.48	7.51	5.894	94.7	vvs
1 0 0	14.10	14.14	3.155	31.6	ms
0 0 2	15.05	15.16	2.947	3.1	vvw
1 0 1	16.07	16.09	2.782	11.5	vvs
1 0 $\bar{1}$				100.0	
1 0 2	20.93	20.97	2.154	69.5	ms
0 0 3	23.10	23.10	1.965	5.4	vw
1 1 0	24.98	25.04	1.822	29.8	m
1 1 1	26.25	26.29	1.740	22.0	mw
1 0 3	27.46	27.53	1.668	20.2	mw
1 0 $\bar{3}$				2.8	
2 0 0	29.17	29.25	1.577	4.3	vw
1 1 2	29.85	29.84	1.549	3.4	vvw
2 0 1	30.32	30.30	1.524.	14.9	mw
2 0 $\bar{1}$				2.1	
0 0 4	31.42	31.55	1.473	4.8	vw
2 0 2	33.54	33.66	1.391	16.4	mw
1 1 3	35.21	35.25	1.336	9.0	w
1 0 4		35.27	1.335	4.9	
2 0 3	38.75	38.81	1.230	1.0	vw–w
2 0 $\bar{3}$				7.2	
2 1 0	40.16	40.28	1.192	3.3	vw
0 0 5	40.68	40.84	1.179	1.0	vvw
1 2 1	41.16	41.27	1.169	12.4	mw
2 1 1				1.7	
1 1 4	42.21	42.29	1.146	12.9	w
2 1 2	44.09	44.22	1.105	16.0	m
1 0 5		44.28	1.104	0.7	
1 0 $\bar{5}$		44.28	1.104	5.3	

0022–2461/79/102516–04 $02.40/0